Teknik Bilimler Dergisi
Cilt 14, Sayı 2, S. 42-58, Temmuz 2024

Araştırma Makalesi

TECHNICAL SCIENCES
e-ISSN:2146-2119

Journal of Technical Science
Volume 14, No. 2, pp. 42-58, July 2024

Research Article

Determination Of Weld Thickness In Hollow Section Connection Under Local Buckling Effect

. İlyas Devran ÇELIK[1], Mehmet FENKLİ[2], Mustafa SİVRİ[3*], Tuğrul TULUNAY[4]

[1] Süleyman Demirel Ünveristesi, Mühendislik Fakültesi, İnşaat Mühendisliği Bölümü, Isparta, Türkiye, (ORCID: 0000-0001-9011-4041), devrancelik@sdu.edu.tr
[2] Isparta Uygulamalı Bilimler Üniversitesi, Teknoloji Fakültesi, İnşaat Müh. Bölümü, Isparta, Türkiye (ORCID:0000-0001-7660-9849) mehmetfenkli@isparta.edu.tr.
[3*] Isparta Uygulamalı Bilimler Üniversitesi, Teknik Bilimler MYO, İnşaat Bölümü, Isparta, Türkiye, (ORCID: 0000-0002-2756-5357), mustafasivri@isparta.edu.tr.
[4] Süleyman Demirel Ünveristesi, Mühendislik Fakültesi, İnşaat Mühendisliği Bölümü, Isparta, Türkiye, (ORCID: 0000-0002-1849-8690), tugrultulunay@gmail.com.

(İlk Geliş Tarihi 02.11.2023 ve Kabul Tarihi 07.08.2024)

(**DOI:** 10.35354/tbed.1384943)

ATIF/REFERENCE: Çelik İ. D., Fenkli, M., Sivri, M., & Tulunay, M. (2024). Determination Of Weld Thickness in Hollow Section Connection Under Local Buckling Effect. *Teknik Bilimler Dergisi*, 14 (2), 42-58.

Abstract

Hollow section profiles are widely used in the structural steel industry. An important point to take into consideration in such connections is the continuous transfer of internal forces from element to element. One of the measures taken to ensure this continuity is to use end plates. The connection between plates and elements is mainly provided by welds. The aim of this study is to determine an optimum weld thickness for connections subjected to local buckling of box-beam-columns under bending. Corner and circular fillet welds were used to join the designed plates with box columns and beams. Hollow section profile connections were experimentally studied in the Steel Structure Laboratory of the Department of Civil Engineering of Süleyman Demirel University. Results were used to develop numerical models. Ansys Workbench was used in numerical models to analyze the corner welds of different thicknesses and lengths depending on plate dimensions and to examine their behavior. It was detected that in corners which the stress concentrations occur, weld thickness greatly impacts the structural behavior.

Keywords: Hollow section beam-column connections, calculation and construction principles 2016, design of steel structures, welded connections under local buckling, weld thickness.

Kutu Kesitli Birleşimlerde Kaynak Kalınlığının Bölgesel Burkulma Davranışına Etkisi

Öz

Kutu kesitli profiller yapısal çelik endüstrisinde yaygın olarak kullanılmaktadır. Bu tür bağlantılarda dikkat edilmesi gereken önemli bir nokta iç kuvvetlerin elemandan elemana sürekli olarak aktarılmasıdır. Bu sürekliliğin sağlanması için alınan önlemlerden biri de ek plakaların kullanılmasıdır. Plakalar ve elemanlar arasındaki bağlantı esas olarak kaynaklarla sağlanır. Bu çalışmanın amacı, eğilme altında yerel burkulmaya maruz kalan kutu kolon- kiriş birleşimleri için optimum kaynak kalınlığının belirlenmesidir. Tasarlanan plakalar, köşe ve dairesel köşe kaynaklarla kutu kolon-kiriş birleşimlerinde kullanılmıştır. Kutu profil bağlantıları Süleyman Demirel Üniversitesi İnşaat Mühendisliği Bölümü Çelik Yapı Laboratuvarı'nda deneysel olarak incelenmiştir. Sonuçlar sayısal modeller geliştirmek için kullanılmıştır. Plaka boyutlarına bağlı olarak farklı kalınlık ve uzunluktaki köşe kaynaklarının analiz edilmesi ve davranışlarının incelenmesi amacıyla sayısal modellerde Ansys Workbench program kullanılmıştır. Gerilme yığılmalarının yoğunlaştığı köşe noktalarda kaynak kalınlığının yapı davranışını büyük ölçüde etkilediği görülmektedir.

Anahtar Kelimeler: Kutu kesit kiriş-kolon birleşimleri, hesap ve yapım prensipleri 2016, çelik yapıların tasarımı, yerel burkulma altında kaynaklı birleşimler, kaynak kalınlığı.

1. INTRODUCTION

Hollow section profiles are widely used in the structural steel industry in Turkey and in other countries. Cross-sectional properties of hollow section profiles make the connection details of these types of profiles different from those of other hot-rolled ones. The main reason for this is that they are closed section and cold-formed beams. This changes the connection details and urges designers to take additional measures depending on the internal forces of the system behavior. Unwanted deformations, and sudden capacity loss and brittle behavior due to those deformations are observed unless additional measures are taken for connections designed using hollow section profiles. There are many studies that address the prevention of this situation.

Easterling and Gonzales (1993) used three types of steel elements (flat plates, gusset plates and U profiles) and three types of weld configurations to investigate shear lag effects in elements and connections under tensile load. They analyzed the design conditions of the steel elements according to the existing AISC specifications. Twenty-seven specimens produced using welded connections were loaded and tested to failure. Korol (1996) investigated shear lag effects under the tensile loads of welded, slotted connections commonly used in closed section members. He analyzed the effects of weld length, weld distance, and other parameters on connection strength and behavior. 18 specimens were experimentally tested. Fracture was observed in 11 specimens due to block shear failure and in 7 specimens due to shear lag. Cheng et al. (1998) conducted endurance tests on 9 specimens with three different tube sizes and four weld lengths. Fracture was observed in 7 specimens due to ductility while deformation was observed in 2 specimens starting at the weld. Depending on plate orientations and connection types, Zhao et al. (1999) investigated the behavior of longitudinal fillet welds of high-strength (fy=450 MPa) cold-formed rectangular hollow section box profiles with a thickness of less than 3 mm. They analyzed the effect of load conditions, end return welds, and box profile-plate orientation on weld strength. Cheng and Kulak (2000) examined shear lag effect in end regions of closed-section tensile members welded to the gusset plate. 9 different test specimens with 3 different cross-sections and different weld lengths were prepared. An elasto-plastic model was developed using material properties to numerically analyze the connections. It was argued that ductility might decrease if end return weld is performed. Willibald et al. (2004) compiled previous experimental and numerical studies and compared them with connection details developed for welded and slotted connection of tube profiles. Four of the six specimens failed by shear lag, one failed due to block shear tear-out and one failed due to both shear lag and block shear tear-out. Ovalization was observed in all specimens before failure. Taking into account weld length, element length and weld symmetry, Humphries and Birkemoe (2004) experimentally examined the behavior of various sections under tensile load. Ling et al. (2006) investigated shear lag failure in plate welded connections of VHS (Very High Strength) steel tubes. All 16 specimens failed by shear lag and their final strength was determined. Willibald et al. (2006) performed compressive force and tensile force tests on 13 gusset plate elliptical section members. Experimental study results were compared with current design procedures and recommendations of other studies. The effect of connection length, location of the profile section on the plate and distances between welds were taken into account in the test specimens. Abi-Saad and Bauer (2006) analyzed the shear lag effect causing a reduction in strength of steel tension members and adopted an analytical approach to evaluate strength reduction calculations. The approach is based on the assumption that, similar to the Whitmore concept, forces along inclined lines in member ends can be used in connection plates. They illustrated the method with examples for elastic, plastic and ultimate stress conditions on a basic weld. Martinez-Saucedo et al. (2006) tested 8 specimens with 3 different types of connections under axial tension and pressure loads, and used the finite element method (ANSYS) for analysis. Martinez-Saucedo et al. (2008) examined the behavior of plate end connections of closed-section members under inelastic cyclic loading. They conducted tests on three types of connections, including two new modified slotted plate connections, in order to avoid traditional slotted, plate connection and sudden failures. Zhao et al (2008) conducted an experimental study on weld lengths and types of end welds at welded slotted plate connections of square and rectangular hollow section profiles. They tested a total of 30 square and rectangular specimens using 16 separate connection configurations. They addressed the effect of weld location, weld length-section ratios and gusset plates on connections. Zhao et al (2009) performed tests on welded slotted plate connections of square and rectangular hollow section profiles by taking into account weld lengths, profile-plate orientation and weld thickness. They used the finite element method to develop models taking corner strengths of profiles into account, and performed parametric studies using those models, and then compared the test results with standard strength estimates. Martinez-Saucedo and Packer (2009) analyzed limit states to determine the capacity of welded, slotted, plate connections of slotted end hollow structural section connections under tensile loads according to American, Canadian, and European specifications. Schmidt and Morgan (2011) investigated the behavior of tubular steel members and their connections. Three connection details and two types of steel were used, one of which was a conventional semi-rigid steel and the other was a cold-formed rimmed steel.

This study addressed the active force- and local buckling-dependent behavior of welds used in hollow section profile connections under bending and revealed capacity losses due to this behavior. Results were used to determine an optimum weld thickness for box section profiles.

2. Material and Method

This study investigated the behavior of welds depending on local deformations in welded connections of hollow section profiles under bending and analyzed the effect of welds on nodal point capacity. Box section joints were experimentally studied in the Steel Structure Laboratory of the Department of Civil Engineering of Süleyman Demirel University. Results were used to develop numerical models, which were then used to calibrate the numerical models. Based on the calibrated numerical models, the same connections were re-analyzed for different weld thicknesses in order to reveal the behavior of the weld under possible deformations. Then, an optimum weld thickness for welds used in this type of connections was determined.

Models were developed based on specimens used in an experimental study. RHS 200.200.5 mm box beam column and RHS 150.200.4 mm rectangular hollow section beams were welded to obtain specimens. The connection was rigidized with an end plate to avoid possible local deformations on the column under cyclic and statically incremental loads. In this type of

connections, the operation of the end plate and column section as a whole under bending is of great importance for joint rigidity. Although the plate and column head cooperate partially in the pressure zone, especially under bending, they behave independently of each other in the tensile zone. For this reason, welding gaps were opened in the end and body regions on the end plate, and fillet welding as well as peripheral welding was performed to join the plate and the column.

Figure 1 shows the layout and images of the end plate welded to the column. The end plate designed as a rigidizing plate has been geometrically designed to surround the column to control deformation in the column upper end and panel area. The connection was confined to the plate edge and joined under the plate using the column holes over the column head along the plate in order to prevent the plate from moving independently of the column profile. Figure 1 shows the dimensions of the plate. Pv is the longitudinal length of the plate with 300, 350, 400 mm. Ph is the horizontal length of the plate, which completely covers the column face, and therefore, the value is constant (200 mm). This value of the plate is included in the study as 50, 75 and 100 mm. The diameter of the fillet welds allowing the plate to cooperate with the column head at the connection is 15 mm, and they were placed at a distance of 50 mm on the plate and 100 mm on the edge of the plate.

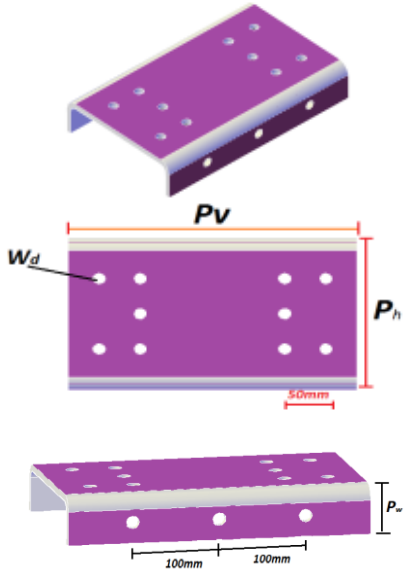

Figure 1. End plate layout and views

The fillet weld dimension parameters for the experimental specimens were scaled based on the joint geometry, and no calculation was performed. However, the parameters in this study were calculated by considering the specifications of Regulation 2016 on Design, Calculation and Construction Principles of Steel Structures, and numerical models were developed and analyzed for the new values. The numerical models were divided into 9 main groups taking into account plate dimensions. These groups were divided into subgroups, including the changes in weld thickness and fillet weld dimension parameters of the connection. Table 1 shows the 9 numerical models and their nomenclatures.

In graphs and tables, experimental models are presented with D and numerical models are presented with S.

Table 1. End plate dimensions used in numerical models

Numerical Model No	Column (mm)	Beam (mm)	End Plate	Plate Thickness t (mm)	Pw (mm)	Pv (mm)	Ph (mm)	Weld Thickness a(mm)
SM-1	200*200*5	150*200*4	YES	8	50	300	200	3
SM-2	200*200*5	150*200*4	YES	8	75	300	200	3
SM-3	200*200*5	150*200*4	YES	8	100	300	200	3
SM-4	200*200*5	150*200*4	YES	8	50	350	200	3
SM-5	200*200*5	150*200*4	YES	8	75	350	200	3
SM-6	200*200*5	150*200*4	YES	8	100	350	200	3
SM-7	200*200*5	150*200*4	YES	8	50	400	200	3
SM-8	200*200*5	150*200*4	YES	8	75	400	200	3
SM-9	200*200*5	150*200*4	YES	8	100	400	200	3

Figure 2 shows the variance of the dimensional parameters determined for the fillet welds in the numerical models. Table 2 shows the model nomenclature for these variables.

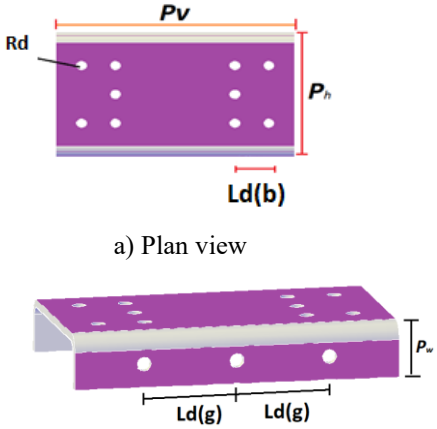

a) Plan view

b) Frontal view

Figure 2. Variables defined for end plate fillet welds

The models were analyzed using the Ansys WorkBench V15.0 finite element analysis software. The models were analyzed using the Ansys WorkBench V15.0 finite element analysis software. Ansys can perform nonlinear analysis for both material and geometry. For this reason, profile, weld and bearing plates were modeled considering the nonlinear material properties. Column, beam, loading arm and bearing plates were modeled as "shell" elements, while rider plate and welds were modeled as "solid" elements. Figure 3 shows the shape of the numerical model.

Table 2. Sub-groups based on weld thickness and fillet weld dimensions

	Numerical Model No	Rd (mm)	Ld(b) (mm)	Ld(g) (mm)	Weld Thickness a (mm)	End Plate	Plate Thickness t (mm)	Pw (mm)	Pv (mm)	Ph (mm)
1	SM-1/3-D15	15	50	100	3	YES	8	50	300	200
2	SM-1/3-D16	16	64	100	3	YES	8	50	300	200
3	SM-1/6-D15	15	50	100	6	YES	8	50	300	200
4	SM-1/6-D16	16	64	100	6	YES	8	50	300	200
5	SM-2/3-D15	15	50	100	3	YES	8	75	300	200
6	SM-2/3-D16	16	64	100	3	YES	8	75	300	200
7	SM-2/6-D15	15	50	100	6	YES	8	75	300	200
8	SM-2/6-D16	16	64	100	6	YES	8	75	300	200
9	SM-3/3-D15	15	50	100	3	YES	8	100	300	200
10	SM-3/3-D16	16	64	100	3	YES	8	100	300	200
11	SM-3/6-D15	15	50	100	6	YES	8	100	300	200
12	SM-3/6-D16	16	64	100	6	YES	8	100	300	200
13	SM-4/3-D15	15	50	100	3	YES	8	50	350	200
14	SM-4/3-D16	16	64	100	3	YES	8	50	350	200
15	SM-4/6-D15	15	50	100	6	YES	8	50	350	200
16	SM-4/6-D16	16	64	100	6	YES	8	50	350	200
17	SM-5/3-D15	15	50	100	3	YES	8	75	350	200
18	SM-5/3-D16	16	64	100	3	YES	8	75	350	200
19	SM-5/6-D15	15	50	100	6	YES	8	75	350	200
20	SM-5/6-D16	16	64	100	6	YES	8	75	350	200
21	SM-6/3-D15	15	50	100	3	YES	8	100	350	200
22	SM-6/3-D16	16	64	100	3	YES	8	100	350	200
23	SM-6/6-D15	15	50	100	6	YES	8	100	350	200
24	SM-6/6-D16	16	64	100	6	YES	8	100	350	200
25	SM-7/3-D15	15	50	100	3	YES	8	50	400	200
26	SM-7/3-D16	16	64	100	3	YES	8	50	400	200
27	SM-7/6-D15	15	50	100	6	YES	8	50	400	200
28	SM-7/6-D16	16	64	100	6	YES	8	50	400	200
29	SM-8/3-D15	15	50	100	3	YES	8	75	400	200
30	SM-8/3-D16	16	64	100	3	YES	8	75	400	200
31	SM-8/6-D15	15	50	100	6	YES	8	75	400	200
32	SM-8/6-D16	16	64	100	6	YES	8	75	400	200
33	SM-9/3-D15	15	50	100	3	YES	8	100	400	200
34	SM-9/3-D16	16	64	100	3	YES	8	100	400	200
35	SM-9/6-D15	15	50	100	6	YES	8	100	400	200
36	SM-9/6-D16	16	64	100	6	YES	8	100	400	200

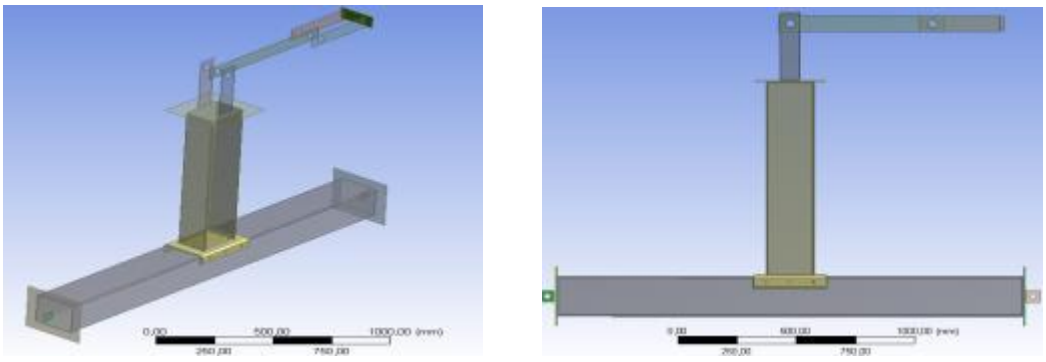

a) Numerical model general view b) Numerical model sectional view

Figure 3. ANSYS numerical model general views

For analysis results to be real-like, the quality of the member's mesh (finite element) must be high in the modeling phase. In order for this mesh quality to be high, the mesh geometry should be as smooth as possible and reach enough numbers. If the mesh quality is low, load transfer becomes discontinuous and results become less accurate. if mesh, that is, the finite element fragmentation, is performed too often, the result will not change and the resolution time will be longer, as the number of elements and the number of nodes will increase. For this, it is necessary to perform meshing in an appropriate range. The mesh range suitable for Ansys was determined to range from 24000 to 25000 and

analysis was performed within this range. Figure 4 shows the desired mesh structure.

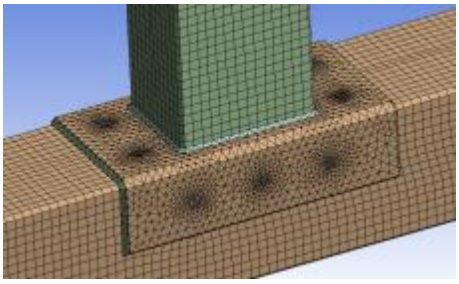

a) Nodal point mesh model

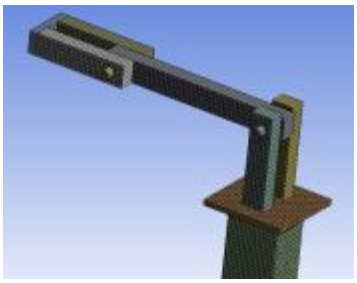

b) Mesh model

Figure 4. Ansys model meshed model general view

The finite parts were defined as shell and solid by the software. The definition of an element as solid or shell in the software depends on its geometry. In this context, the finite parts in the weld and end plate with variable forms were introduced as solid to the software. The other parts with a uniform (rectangular, square, etc.) form were defined as shell elements.

The study aimed to determine an optimum weld thickness for a connection exposed to local buckling in the column and beam under bending. Therefore, the numerical model focused more on the weld member than on the column and beam, and their behavior was evaluated. Many studies have ignored welds in such connections and directly connected the structural members together. The models in this study took the weld into account and tried to determine an optimum weld thickness. In other words, this study examined the possible deformations in welds. Estimates of these deformations were evaluated performing stress analysis on the welds.

In the models, fixed bearings which are free to rotate round the Z axis on the reaction wall connections of bearings but are otherwise limited in the other directions were defined. This was generated using the "remote displacement" command in the Ansys.

In order for the model to behave rigidly, the joints were connected to each other using the "bonded" command, which bonds the two surfaces (column-column end plate) to each other. The algorithm for the nonlinear buckling analysis of the model was primarily based on linear buckling, and the optimal buckling mode was determined. Nonlinear numerical analysis was carried out considering the effects of nonlinear materials based on deformation.

Local deformations are observed in the column, beam and cross member at a node point designed using box beam profiles under bending. These deformations in the structural member play a role in the connection exhibiting rigid or semi-rigid behavior. Studies indicate that local buckling effects on the column play an active role in connection behavior. CIDECT and Euro Code 3 Part 8 have addressed this extensively. These regulations have established criteria for rigid and semi-rigid definition of such connections and developed empirical formulas based on some coefficients calculated using column and beam dimensions for the determined stiffness range. Ultimate bearing capacities of connections have been determined using those formulas. Figure 5 shows the connection in CIDECT and Eurocode.

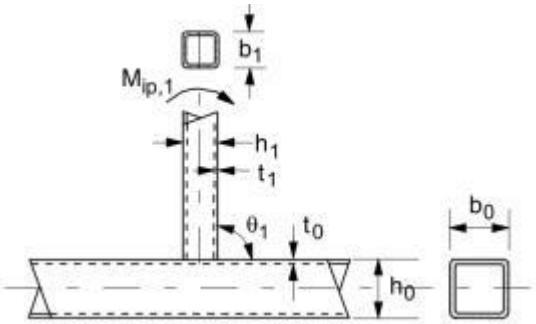

Figure 5. Connections and dimensional parameters used in connections in CIDECT and Eurocode

The coefficients in the design guides mentioned above; the beam width/column width ratio, β, and the column wall thickness/column depth ratio, γ, are proportional coefficients. Joint rigidity was defined based on these coefficients. Depending on the value of the factor β, which plays a key role in determining rigidity, deformations on the column are observed in the head or body or both. In general terms, when β = 1.0, deformation is observed in both the head and body of the column, and the joint exhibits rigid behavior. When β <0.9, the deformation is limited only to the column head, and the joint exhibits semi-rigid behavior. The definition and accepted formulations here are based on the dimensional parameters of the structural member in question and on possible deformation regimes. However, in this type of welded connections, welds connecting the joints together should preserve the integrity of the weld and be free of any discontinuities that may occur with any fracture or failure in order for the accepted formulations to be effective. This study demonstrates the behavior of the welds, which are used in these types of connections under bending, and examines their effect on capacity.

Welding is a thermal connection method which causes changes in the chemical structure of the structural member that it connects. The most significant change in these types of thermally connected joints takes place on the carbon structure of the material, which causes the material to become brittle, and thus, lose its ductility, and results in undesired and sudden deformations. This applies to all weld connections. Therefore, all regulations in the literature define safety coefficients for welds separately from those of other connection types. However, the definitions for welds assume that the connected member maintains its section integrity under the influence of internal forces and that the connection is rigid. However, the occurrence of local buckling in connections where box beam profiles are used, particularly in the joint area, brings about additional stresses which are not calculated for welds. For this reason, dimensional parameters such as weld thickness and length defined for welds are insufficient. This study evaluated the weld dimension parameters defined in the literature and determined the ideal dimension parameters for the numerical model.

3. Research Findings and Discussion

Analyses were grouped under 9 main models. These models consist of end plates depending on geometrical features varying according to fixed column and on the beam size. This study is about the performance of dimensional variables of connected welds under local deformations. To this end, the 9 main models were divided into 36 sub-models under different combinations of dimensions and geometric layout of welds used in the connections. At this point, two different analyses were performed for the end plate-column connection girth seams corner weld thickness and beam-end plate girth seams corner weld thickness. The former is a = 3 mm, which is the value calculated for such a connection according to the criteria in the Regulation 2016, AISC 360-10 and Euro Code for the Design, Calculation and Construction of Steel Structures. The latter is a = 6 mm, which is defined by the TÜBİTAK 111-M-125 project for this type of connection member and calculated using the $(A_{beam}x1400 = 0,7xl_{weld}xa_{weld}x1100$ formula.

Other parameters included in the study are the fillet welds used to ensure the performance of the end plate together with the column to which it is connected. The first of these are intermediate distances between end plate and fillet weld Ld (b) = 50mm, intermediate distances between body and fillet weld Ld (g) = 100mm, and fillet weld diameter Dd = 15mm, which are the parameters of the experimental specimens used for calibration. The other group values defined for fillets welds are those obtained using the criteria in the regulations. These values are intermediate distances between end plate upper region and fillet weld Ld(b)=64mm, intermediate distances between body and fillet weld Ld(g)=100mm and fillet weld diameter Dd=16mm.

Table 3 shows the mechanical properties of the welds used in numerical analysis. These values are used in modeling of welds in numerical analysis (Values are the factory data for the inert-gas unalloyed welding wire).

Table 3. Mechanical properties of welds used in manufacturing

Yield Stress (kg/mm^2)	Ultimate Stress (kg/mm^2)	Elongation (%)	Elasticity Modulus (kg/mm^2)
46	59	28	21000

The numerical models were calibrated to experimental specimens, therefore, the mechanical properties of the profiles were defined according to the mechanical values of the profiles used in the experiments. For this reason, the steel material properties include the tensile test results of the specimens taken from the experimental specimens of the project 111-M-125. Figure 6 shows the result of the tensile test for the steel used in the specimens.

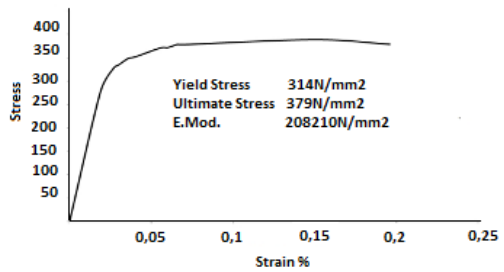

Figure 6. Stress-deformation diagram of tensile test

This study investigates the effect of variation in dimension parameters of welds used in welded box section connections exposed to bending on weld and joint performance. Evaluations were made on the numerical models developed using the results in the experimental models. Figure 7 compares the load-displacement curves obtained from the experimental results for these connections and the results of the models developed using the ANSYS Workbench V15 for the specimens.

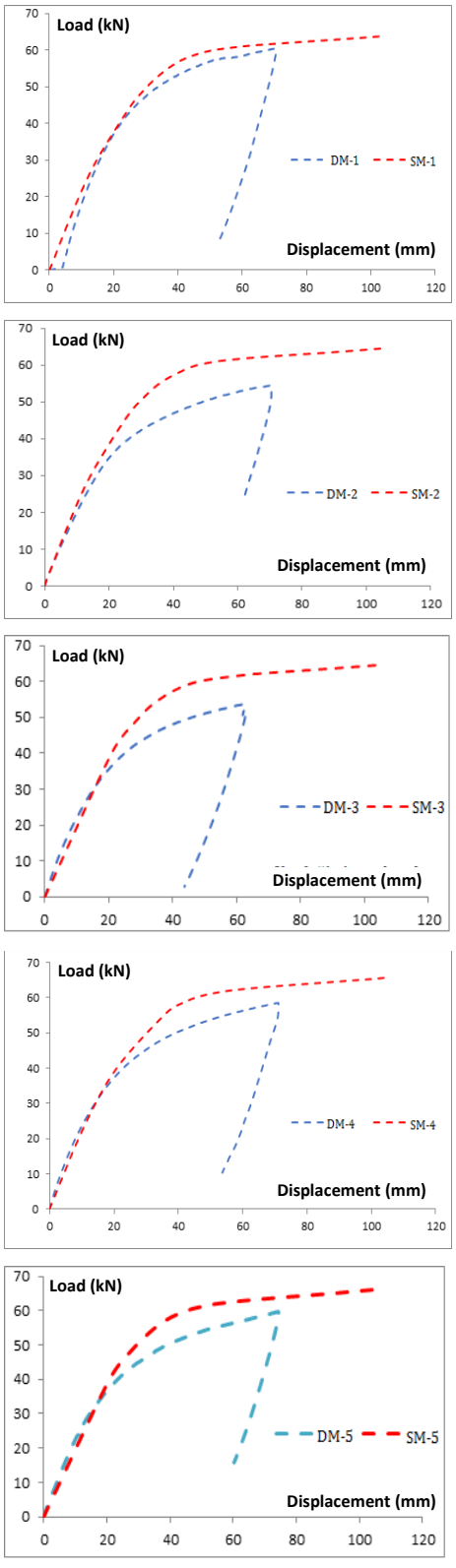

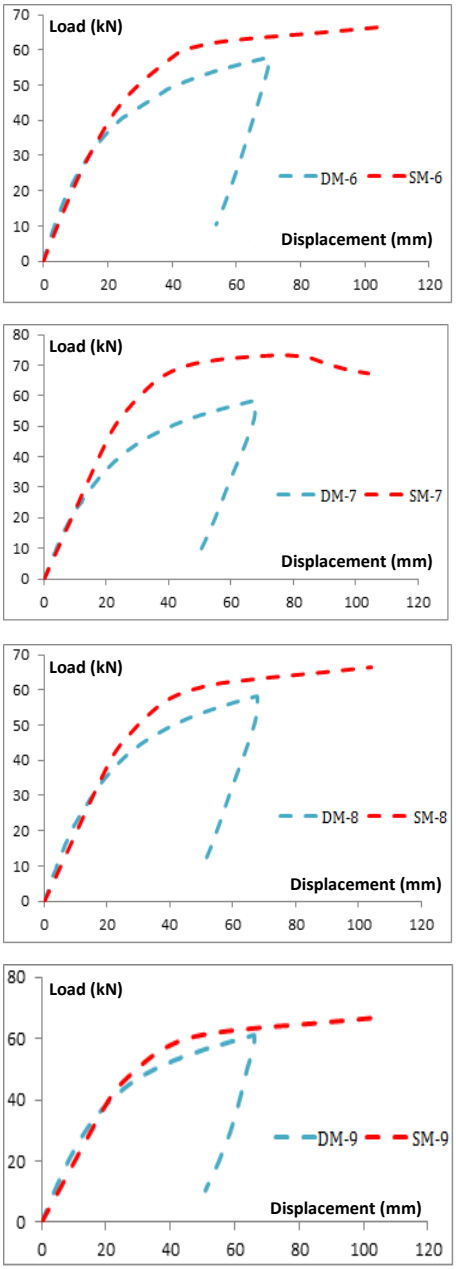

Figure 7. Comparison of load-displacement graphs of experimental and numerical models

The capacity curves in Figure 7 show that the load-displacement values for all the models are particularly in line with the linear boundaries. The differences in some graphs are due to the fact that the beam element became brittle owing to thermally connected weld in the experimental study and that the brittle beam element tore in the boundary line where it was welded using seam welding. The graphs are different because numerical models did not define the embrittlement of the material depending on the thermal effect in this boundary line. However, since the graphics are in harmony in general, the numerical models were verified. The sub models developed based on the subsequent weld dimensions were replicated using these numerical samples.

The local deformations in the 9 main models defined according to the end plate dimensional parameters depended on the dimensions of the plate along the column and its depth. This study discusses the variations in local deformation of welds according to the formation pattern and first explains the deformation algorithm in the connection before interpreting the graphics in this section. The analysis results and stress-deformation distributions obtained according to the results show that similar behaviors are observed for different stress values. For this reason, common results obtained in all items were explained through SM1-3/D15 model data.

The first model, SM1-3 / D15, which differs from the main models due to weld thickness and dimension factors, was analyzed under repetitive cyclic loading using ANSYS Workbench V15. Figure 8 shows the views of the deformed state of the node. When the deformed state is interpreted as a pressure zone and a tensile zone, the column head and body (panel region) move in the same direction in the tensile zone. Thus, internal forces can easily be transferred from the column head to the body. The deformation due to the forces transmitted in the same direction is parallel to each other at the head and body, and the column section properties significantly affect the capacity.

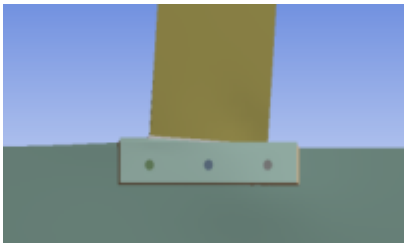

a) Deformed side view

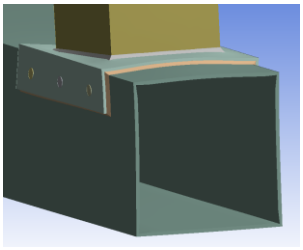

b) Tensile zone views

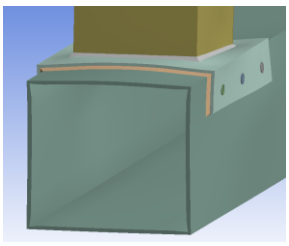

c) Tensile zone views

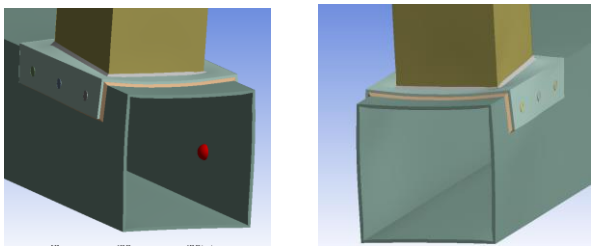

d) Pressure zone views

Figure 8. SM-1 Model post analysis general views

However, the views for the pressure zone in Figure 8 show that the column head plate used the body as a bearing and behaved like a simple beam (membrane behavior), therefore, the cross-sectional capacity was insufficient. In this model, the views of the deformation of the connection were similar in all other models

and it was only that the deformation in term of the stiffness dimension provided by the end plate was more controlled.

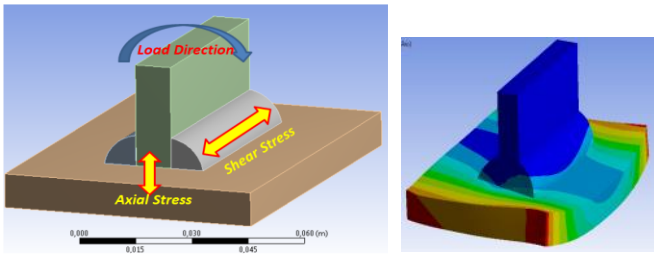

a) Types of stress in corner weld

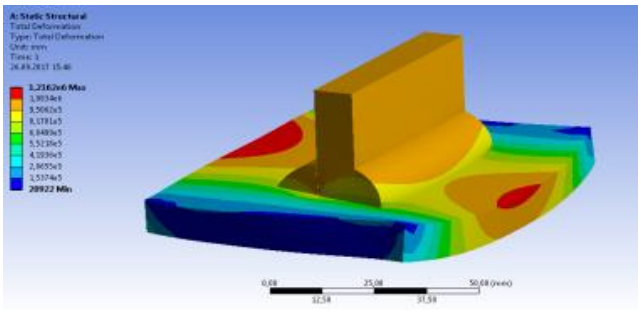

b) Deformed stress distributions

Figure 9. Stress distributions in pressure and tension zones under bending

Figure 9 shows that the behavior of the section in the stress zone and tensile zone is different. The movement of the column and end plate in the tensile zone together also applies to the welds connecting these two elements. The circumferential welds are subjected to extra shear stresses other than normal stresses due to the shape and sequence of the deformations in the column head and body in the stress zone. The next section will interpret the deformation-related behavior of the welds in relation to the graphs obtained from the analyses. The welds in the graphs will be referred to as in Figure 10.

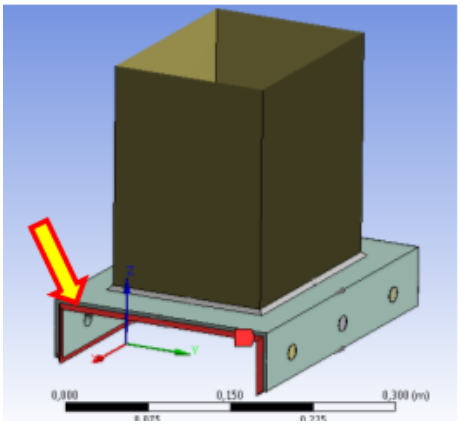

a) Plate circumference corner weld

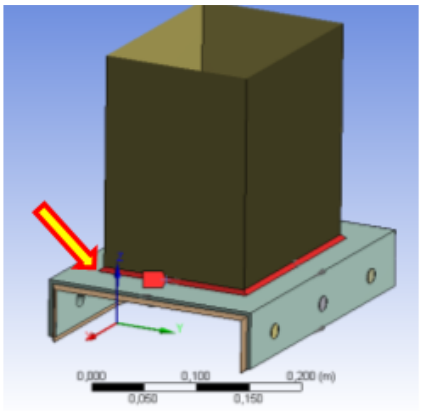

b) Beam circumference corner weld

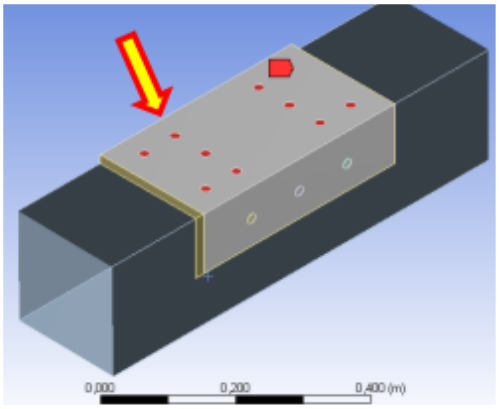

c) Plate head fillet welds

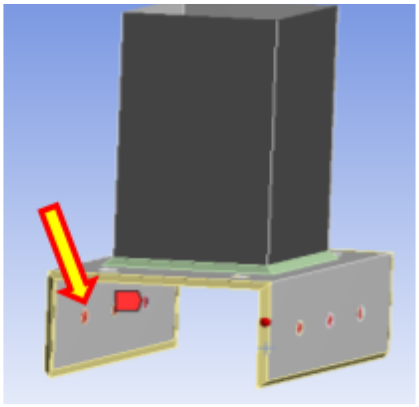

d) Plate body fillet welds

Figure 10. Nomenclature of welds

Figure 11 shows the stress distributions for the deformed state of the circumferential welds connecting the end plate-column and beam-end plate.

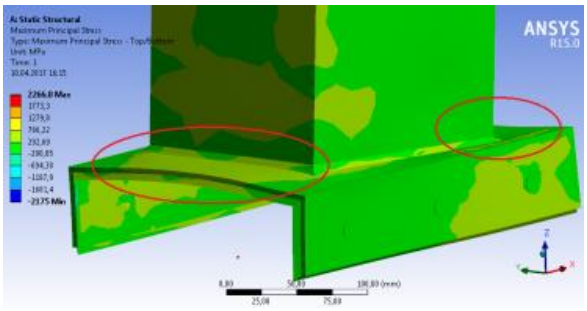

a) Tensile zone stress distribution general view

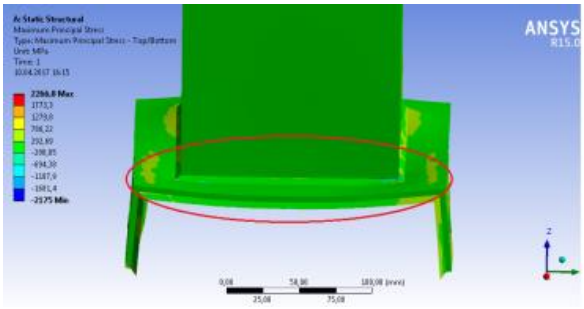

b) Pressure zone stress distribution general view

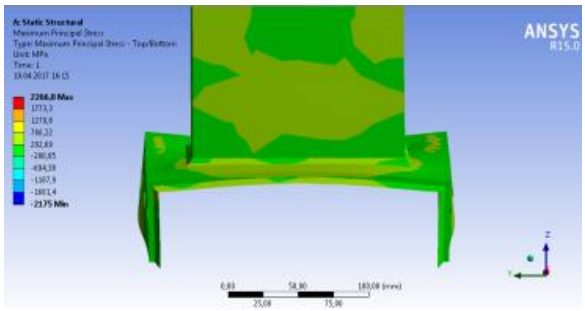

c) Circumferential weld pressure zone stress distribution general view

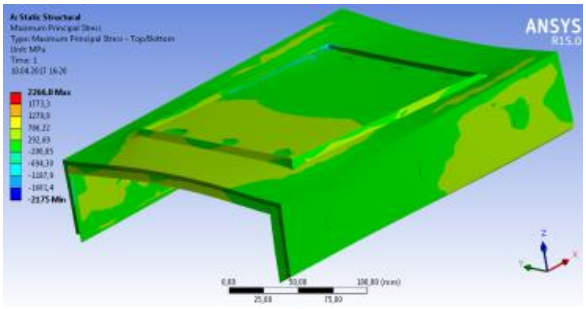

d) Circumferential weld tensile zone stress distribution general view

Figure 11. Deformed welds stress distributions

The graphs show that the stresses in the circumferential welds connecting the plate-column and beam-plate in the tensile zone are in the same direction and continuous as the profiles. However, stresses from the profiles in the stress zone disintegrate in the welds, and even changes signs at the corner points. The change in sign of the stress applied in the same plane and in the same direction in the weld is due to the deformations depending on the membrane behavior of the profile.

Maximum and minimum displacement values of all three axes of the seams and the stress and deformation curves were plotted to examine the effect of the local deformations of the connection on the welds. The data were compared within themselves and with each other.

Figure 12 shows the X direction displacement values of the circumferential weld with a 3 mm and 6 mm thickness of plate-column connection under load. The X direction displacement values of the plate circumferential weld are in the same direction as active force applied to the joint, and the maximum values represent the tensile zone and the minimum values represent the stress zone. The results of the deformed state show that, under bending, local deformation first and effectively occurred in the stress zone, and afterwards, interaction with other regions resulted in deformation, depending on the section effects. This is also apparent in the graphics in this section. The X direction minimum and maximum displacement values in Figure 12 shows that the 3 mm and 6 mm welds are in harmony with each other in the tensile zone but the curves are different from each other in the welds in the stress zones where local deformation occurs and that the shear line is clearly visible in the curve for the 3mm weld.

The end plate-column connection circumferential weld Y direction displacement values in Figure 12 are affected by the local deformation of the column body. Occurrence of the deformation in the plate under confinement effect first in the head and then in the body reduced the interaction of the welds. For this reason, the same results were obtained for the seams with different thicknesses in the displacement analyses in this section. Figure 12 shows the Z direction displacement values of the end plate-column joints circumferential welds. The Z direction is the same as the deformation of displacement values. Using the same structure member and the same rigid plate evened out the deformation of the joint. The curves in the graph show that the 3-mm weld is parallel to the 6-mm weld while the former is below the latter in terms of rigidity.

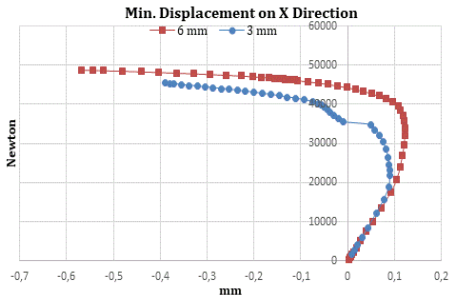

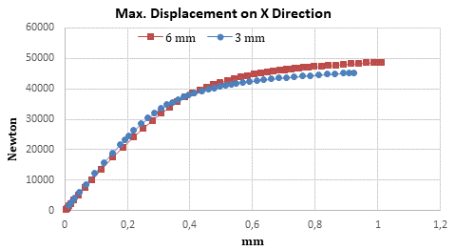

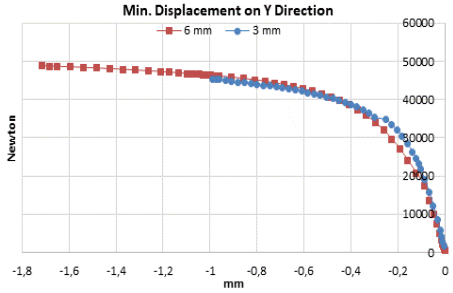

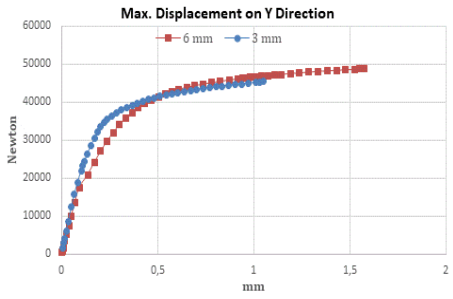

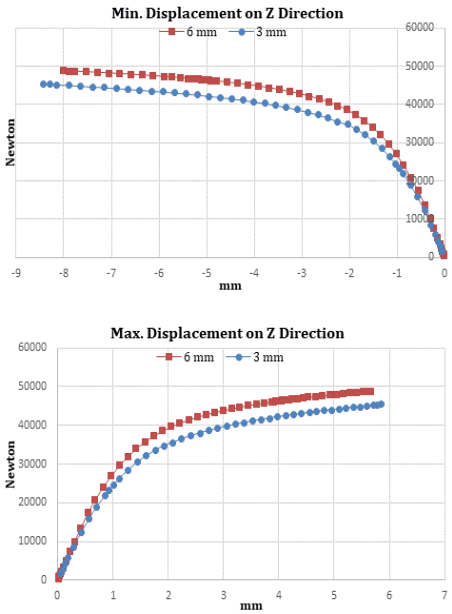

Figure 12. X, Y, Z direction load-displacement graphs of end plate circumferential weld

The plate circumference displacement curves according to numerical analysis results of SM1-3/D15 and SM1-6/D15 models are given as load-deformation and load-stress curves in Figure 13. The graphics clearly show the behavior of the 3mm and 6mm weld in the connection undergoing local deformation. The situation in which the different thicknesses of the welds exhibit the local effect most prominently in the X direction displacement curves has also been confirmed by the deformation curves.

The harmony of the welds in the tensile zone, where the X direction maximum displacements were expressed, was also similar in this section. In the maximum deformation graph, the 6mm and 3mm welds had different values in the linear zone but in the same direction, whereas the deformation rate of the 3 mm weld was higher than that of the 6-mm weld in the plastic zone. In the stress zone where the deformation in the connection was active, the 6 mm weld was able to control the deformation of the joint while the 3 mm weld failed to have enough stiffness and deformed more than the 6 mm weld. The curves of load-stress distributions clearly show that the local deformations had a large effect on the behavior of the weld. The graphs of maximum and minimum stress distributions clearly show that the 6 mm welding stress values were within the linear boundaries whereas the 3 mm welds exceeded the limits.

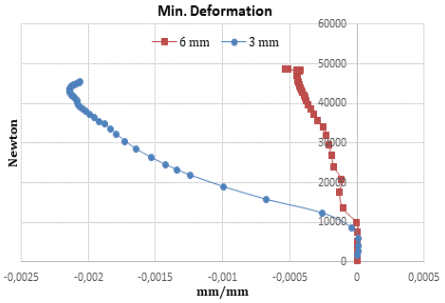

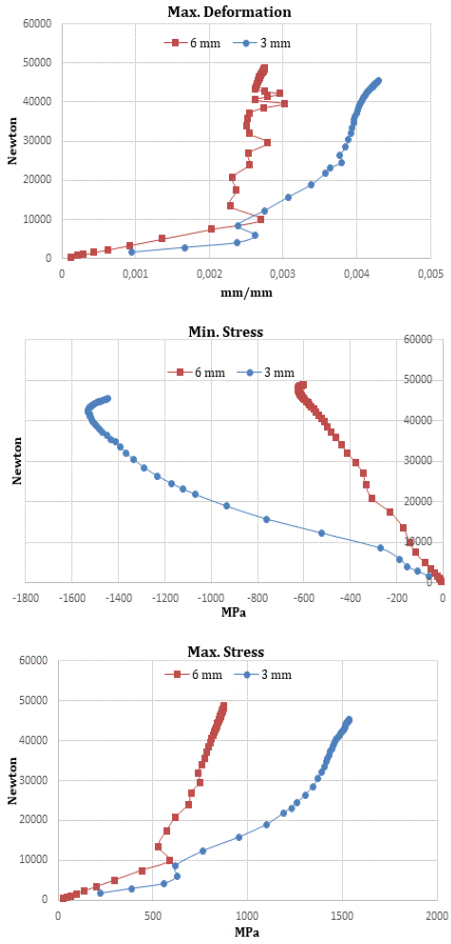

Figure 13. Graphs of plate circumference corner weld

Figure 14 shows the deformation and stress diagrams of the plate head fillet welds used to ensure that the end plates used to prevent possible deformation of the column in the connection under bending was connected to the column head. The fillet weld thicknesses used in the connection were equal to the thickness of the plate (8mm). The diameter was 15mm and the interspace is 50mm. The results in the graph were separated for the plate circumference corner weld thickness. For this reason, the dimensional effect of the plate circumference corner weld did not significantly alter the behavior of those upper fillet welds whereas the results of the 3mm circumferential weld model were less than those of the 6mm circumferential weld model.

Stress values show that the plate head was fully connected to the column head by the fillet weld and that the stresses were in agreement with the deformation and stress distribution in the column head.

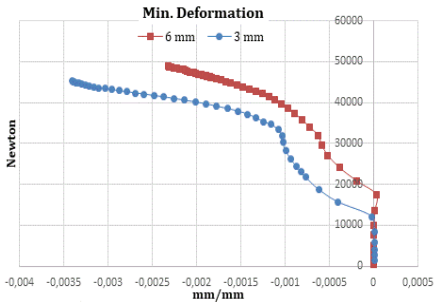

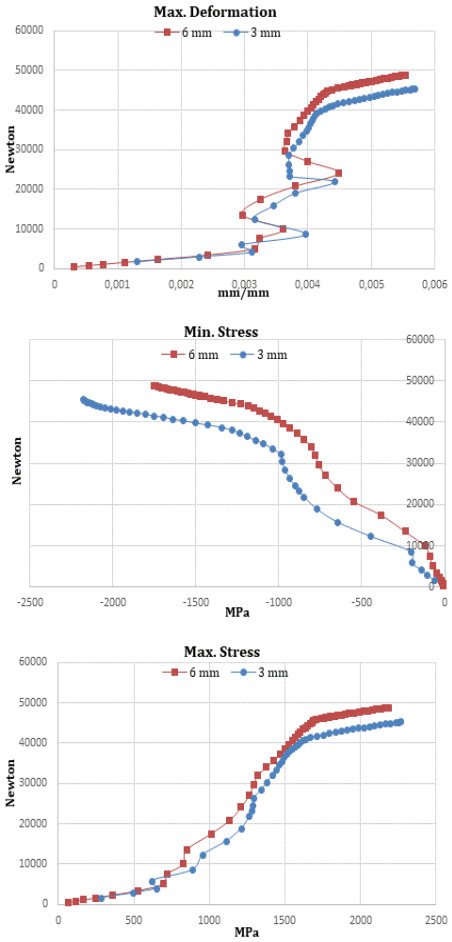

Figure 14. Graphs of plate head fillet welds

Figure 15 shows the plate body fillet weld deformation and stress values. The values yielded similar results to those of the upper fillet weld. The plate body fillet welds provided rigid connection to the column body, deformed along with the column body, and made the stress transfer continuous. The results of the 3 mm circumferential weld model were again less than those of the 6mm circumferential weld model.

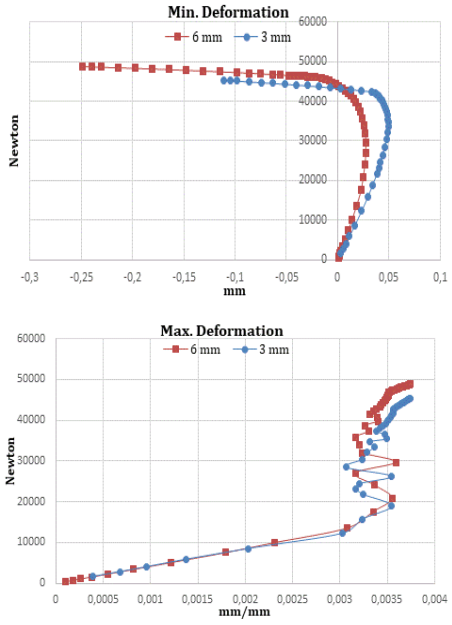

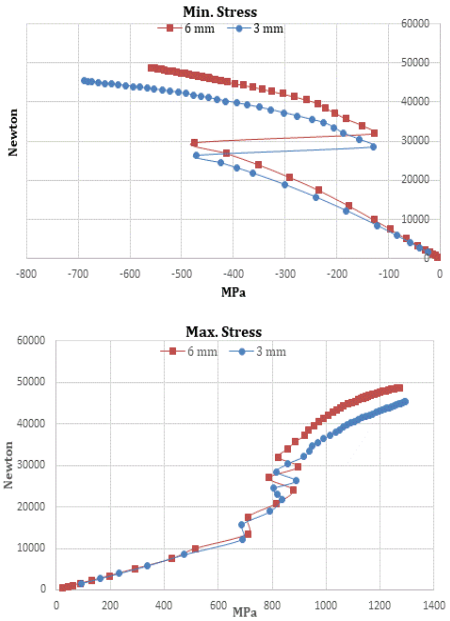

Figure 15. Graphs of plate body fillet welds

In the models, the beam-end plate in the other connection, where the weld thickness was a parameter, was a circumferential weld. The behavior of the weld used in this section was based on the deformation of the end plate to which it was connected. The end plate used to absorb and prevent the deformation of the connection played an active role in the connection and therefore no local deformation was observed at the beam and end plate joint. For this reason, the changes in the welds did not depend on the deformation, and were caused by the brittleness of the thermally connected member under cyclic loading. This is evident in the experimental study, the results of which were used to calibrate the numerical models. This is explained in detail in the 111-M -125 TUBITAK project.

Figure 16 shows the weld displacement values. Deformations in the beam circumferential weld joints were avoided, and therefore, 3 mm and 6 mm welds gave similar results. Circumferential weld Y displacement values are given. This graph shows that the deformations obtained for both thicknesses were similar, and that the 6mm weld was more efficient in terms of capacity and stiffness than the 6mm weld. The graph also shows the displacement values of the circumferential weld Z direction and the results are similar.

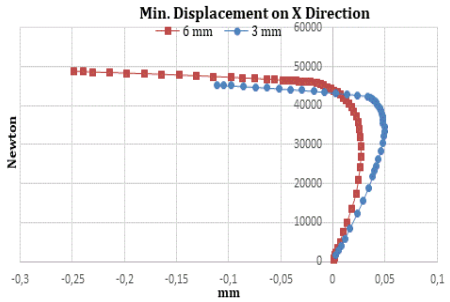

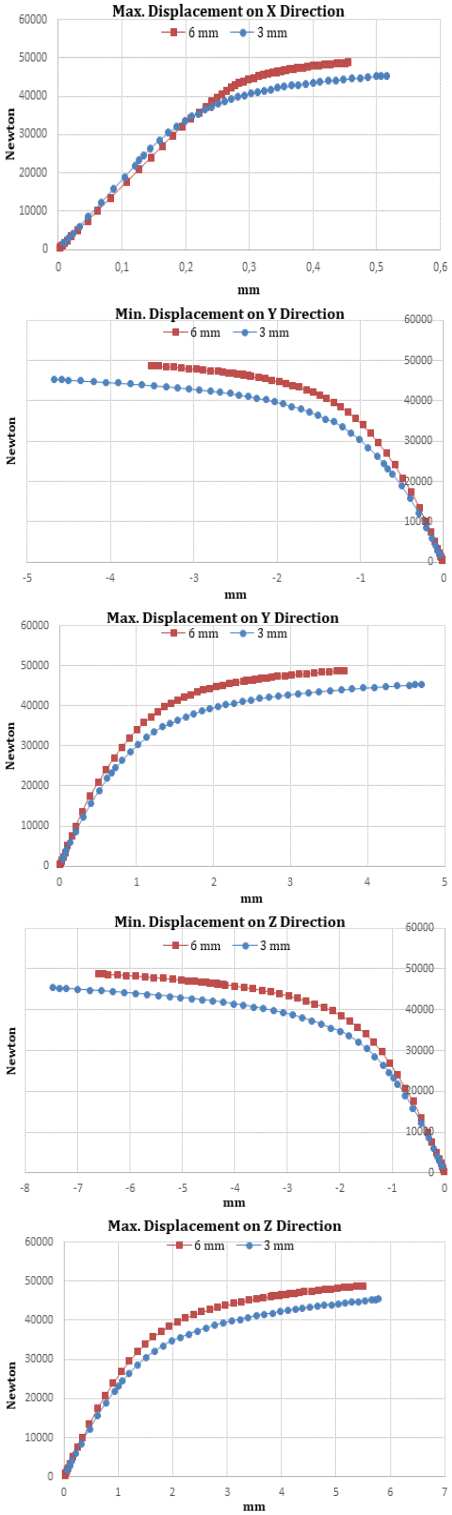

Figure 16. X, Y, Z direction load-displacement graphs of beam-end plate circumferential weld

The results of the load-deformation curves of the beam-end plate circumferential welds are also similar for the load-deformation graphs given in Figure 17. The graphs show that the maximum deformation in the tensile zone was located at a parallel slope for both welds, whereas neither of the welds distorted the weld integrity in the stress zone, where displacements were effective on the seam behavior, and had enough rigidity. In the 3 mm weld, the deformation ratio in the range near the maximum of the load increased markedly, which was due to the fact that the stresses on the weld exceeded the linear boundary. This was the case for the effective area of the 3 mm weld was weaker than that of the 6mm weld. However, this change did not depend on deformation but on stress accumulation. Figure 17 shows the plate circumferential weld load-stress distributions. As can be seen from this section, the 6 mm welds were within the linear boundaries while the 3mm welds had values in the plastic zone.

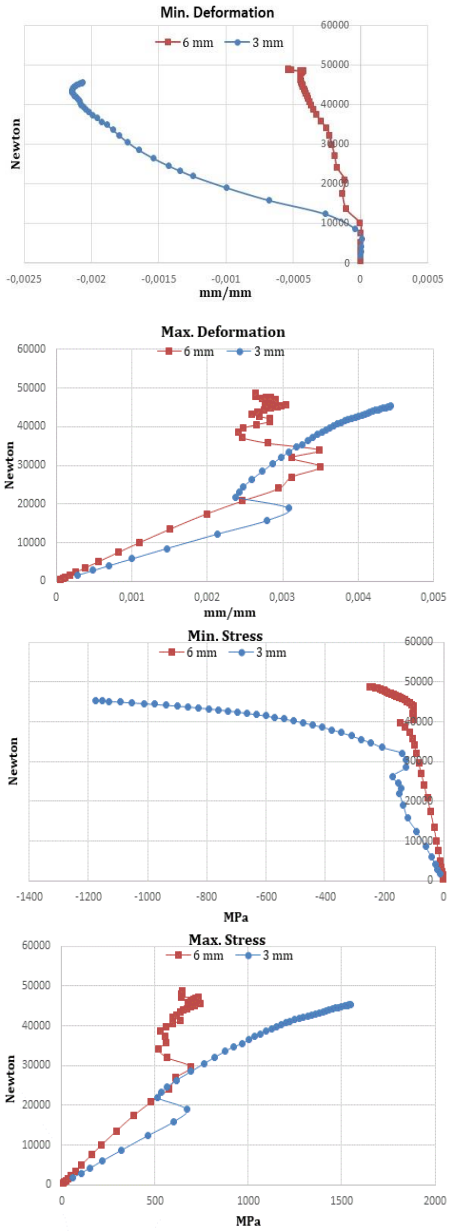

Figure 17. Graphs of beam/end plate circumferential welds

This study analyzed 36 different models under static incremental load using different weld dimension parameters in areas where local deformation was effective in a connection that was rigidized using an end plate. The effect of local deformation of the welds was investigated using weld load-displacement, load-deformation and load-stress curves. The results of the analysis show that the displacement values of deformations under bending were, albeit small differences, similar in all models.

For this reason, instead of analyzing the results of all models separately, the values of model SM1-3/D15 were explained in a representative and comprehensive manner in the previous section. In this section, the load-deformation and load-stress curves demonstrating the behavioral differences in the welds affected by the local deformation of the connection were presented comparatively for the 6 mm circumferential weld. The results show that the deformation of the 3 mm weld was high in the

connection and that it exceeded the linear stress limits and failed to preserve its integrity. For this reason, this section investigated the results for the weld thickness calculated according to the formulation defined in the project of TÜBİTAK 111-M125 for the models used in the study and confirmed the calculated value under deformations.

Figure 18 shows the effect of dimensional change, the activity of which increases in the plate body, on the weld, that is, it comparatively presents the results to express the effectiveness of the welds against deformation in the models in which Group 1 end plate defined in Table 1 was used. According to Figure 18, the effectiveness of the end plate increased and welds exhibited similar behavior in dimensional changes. However, in the case where the smallest plate was used, that is, for the model with effective deformations, the 6 mm weld differed from other models but all welds were within linear boundaries according to stress values.

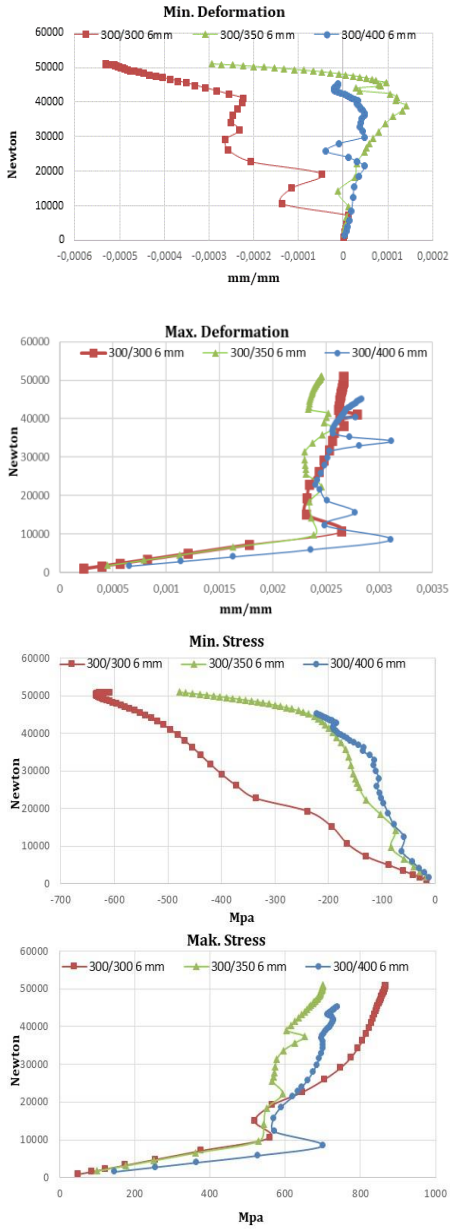

Figure 18. Graphs of plate circumferential weld for Group 1 end plate

Figure 19 shows the deformation and stress values of the beam-end plate circumferential welds in which Group 1 end plate was used. The figure shows that the 6 mm weld was actively used in all end plates and that the stress values on the weld ensured linear boundaries for all results.

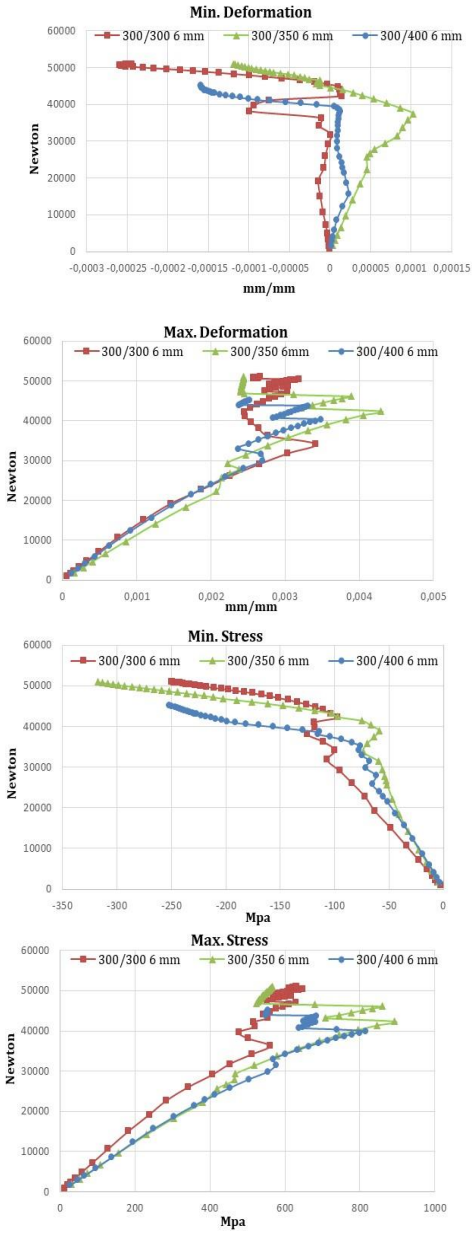

Figure 19. Graphs of beam-end plate circumferential weld for Group 1 end plate

Figure 20 shows the results of the model in which Group 2 plate head was used. The increase in the confinement effect on the column with an increase in the plate size, and confronting the stress and internal forces from the beam in a wider area reduced the deformations on the column to a minimum, which increased the effectiveness of the welds involved in these parts. The stress-deformation graphs in Figure 20 show that the values of the welds in all models overlapped and that all the stresses remained within the linear boundaries.

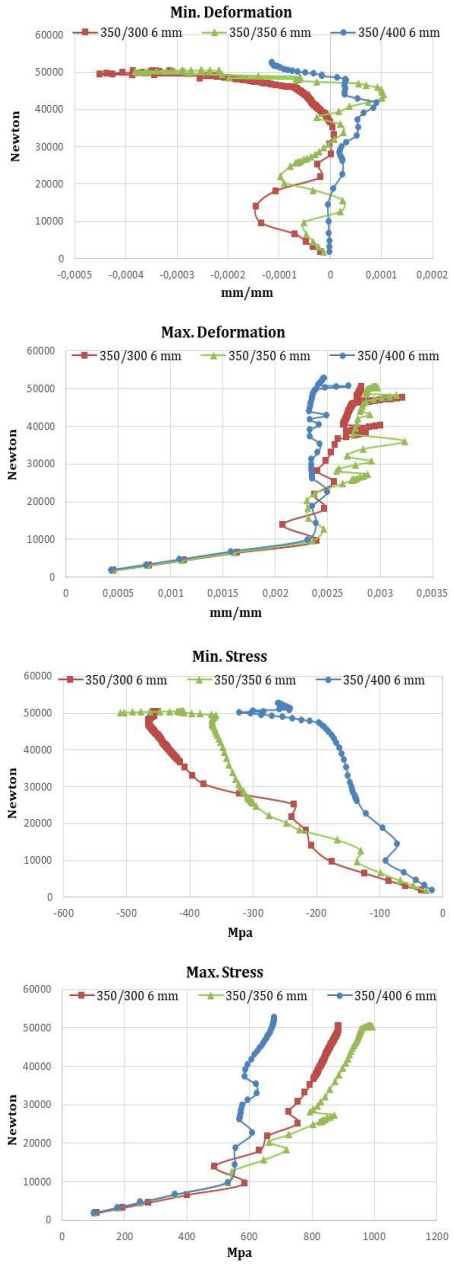

Figure 20. Graphs of plate circumferential weld for Group 2 end plate

The graphs of deformation and stress distributions in Figure 21 belong to the connection point of the beam and end plate. The increase in the confinement effect of the plate on the column positively affected the rigidity of the column and of the plate connected to this column. Therefore, the values of the welds in this section were within the desired limits. The deformations were relatively smaller. The stress values in the linear boundary confirm these results.

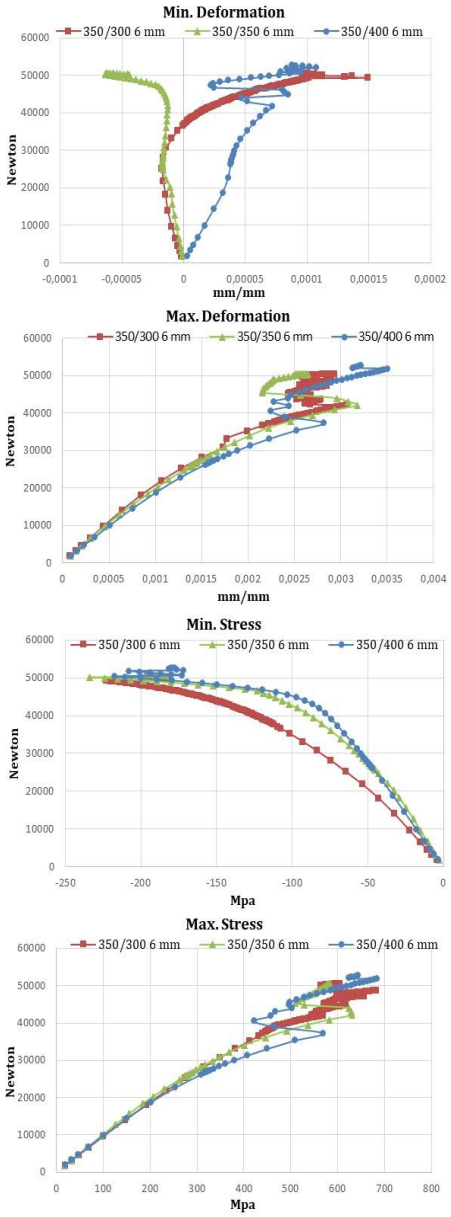

Figure 21. Graphs of beam circumferential weld for Group 2 end plate

The data in Group 3 models in which plates with the largest dimension parameters were used are in agreement with other results. In other words, the increase in the confinement effect of the plate positively affected the welding behavior, the deformation tendencies of the welds decreased, and thus the stress values decreased in the elastic zone. The graphs illustrating this are given in Figure 22.

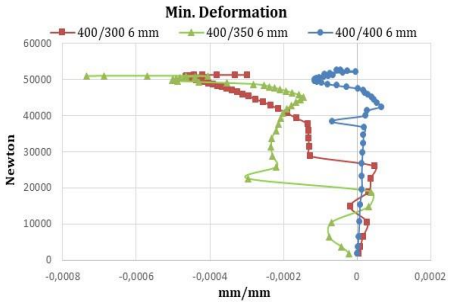

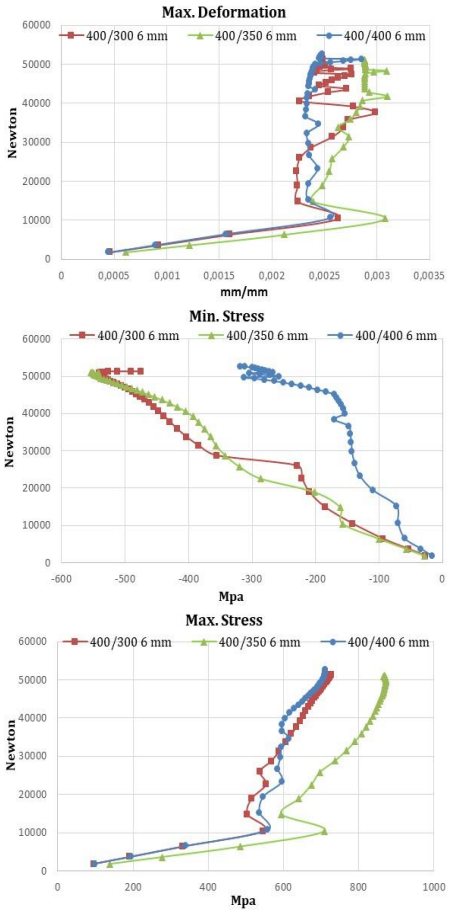

Figure 22. Graphs of plate circumferential weld for Group 3 end plate

In Group 3 models in which plates with the largest dimension parameters were used, the plate confined the column head and body better, thus, preventing deformation and optimizing the weld behavior. This has also been confirmed by the stress and deformation graphs of the circumferential welds. The graphs are given in Figure 23.

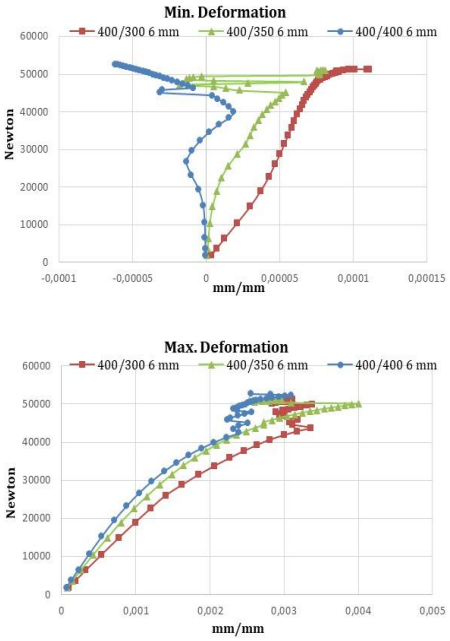

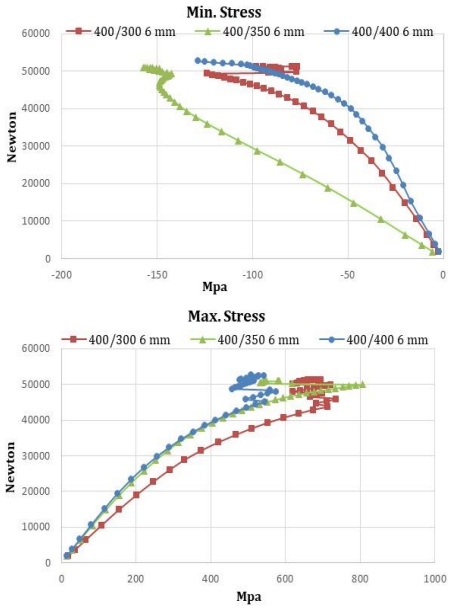

Figure 23. Graphs of beam circumferential weld for Group 3 end plate

Figure 24 analyzed the behavior of the welds in the end plate of the models formed for Groups 1, 2 and 3 end plate with a body length of 50 mm constant and a longitudinal distance of 300, 350 and 400 mm. The most effective result was obtained from Group 1 and 2 plates. However, in terms of stress distributions, the results were similar for all welds.

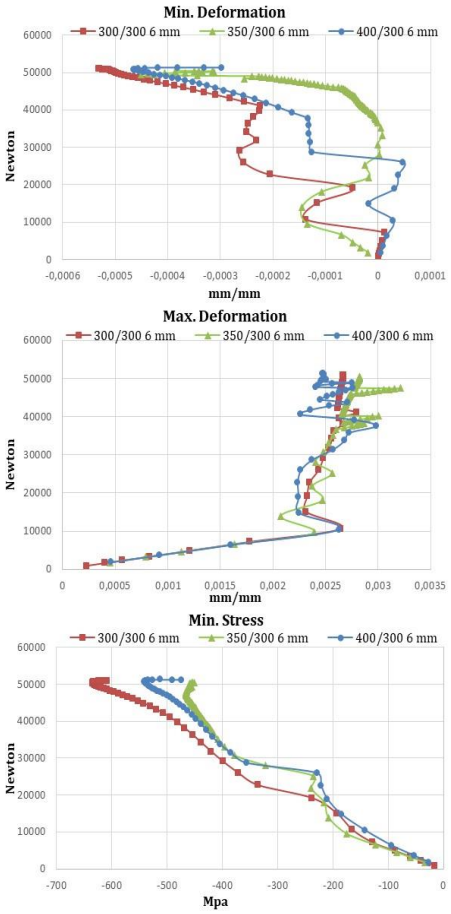

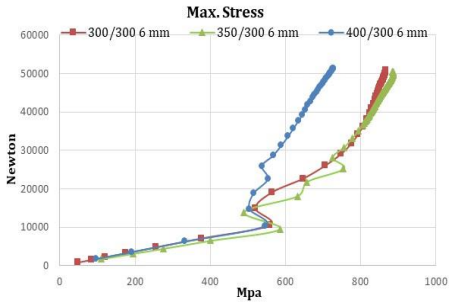

Figure 24. Graphs of plate circumferential weld for length change graphs of 50 mm end plate

Figure 25 analyzed the behavior of the welds in the end plate of the models formed for Groups 1, 2 and 3 end plate with a body length of 75 mm constant and a longitudinal distance of 300, 350 and 400 mm. The most effective result was obtained from Group 1 and 2 plates. However, the results were similar for all welds in terms of stress distributions.

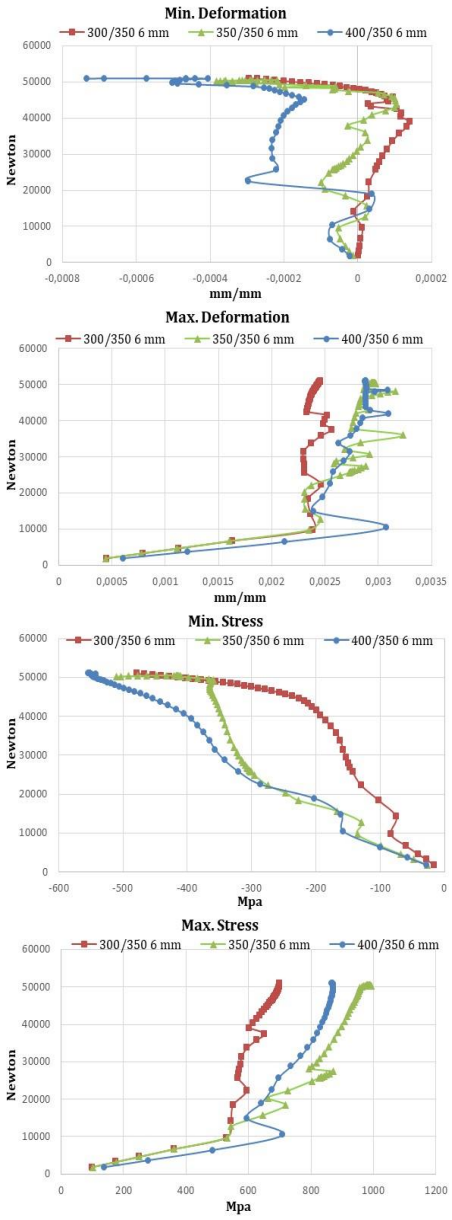

Figure 25. Graphs of plate circumferential weld for length change graphs of 75 mm end plate

Figure 26 analyzed the behavior of the welds in the end plate of the models formed for Groups 1, 2 and 3 end plate with a body length of 100 mm constant and a longitudinal distance of 300, 350 and 400 mm. The greatest confinement effect was in this comparison. The results of the welds for all models were the same in terms of stress and deformation. In other words, every case, where deformations were effectively controlled, positively affected the weld behavior.

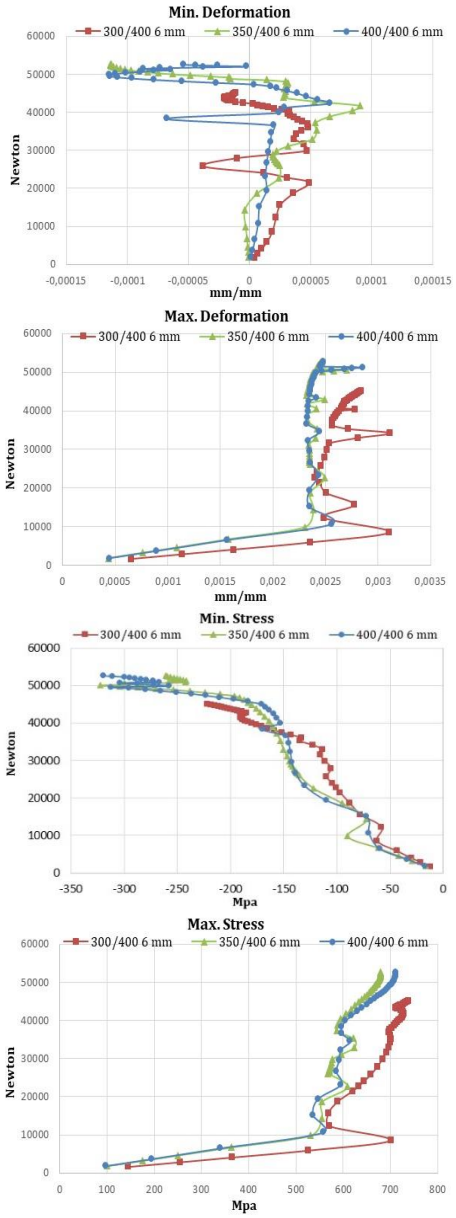

Figure 26. Graphs of plate circumferential weld for length change graphs of 100 mm end plate

4. Conclusion and Recommendations

Section, connection and system integrity must be protected under effective loads so that the capacity value of a structural member composing a joint can be calculated based on the inertia value. This can only be achieved by avoiding local buckling effects on the section and by maintaining the continuity of the connecting parts holding the joint together.

Continuous plates can control the deformation of connections designed using hot-rolled open-section profiles but not in cold-rolled box beam profiles. Some studies have used box fillets, confinement plates and end plates to prevent the local deformation

of box beam connections under bending. In this study, an end plate was used to control the deformation and capacity of the node point. 36 models were developed using welds with different dimension parameters, and they were examined under static incremental load using ANSYS WorkBench. The main determining variable in the models is the circumferential welds that connect the column with the end plate. Based on the relevant specifications, a 3 mm weld thickness calculated for the connection and a 6mm thickness calculated according to the assumptions of TÜBİTAK 111-M125 project were used.

The results show that welds must be protected from additional forces other than the accepted stresses for welds in order to obtain capacity values under the static calculation rules. In other words, in a connection under load, when stress values in welds are supported by additional stresses due to unexpected deformations, weld integrity is compromised and linear boundaries are exceeded and fracture occurs in the welds. The results also show that the optimum weld thickness (3 mm) specified by the regulations is insufficient for this connection. In the models, in which the second value (6mm) was used, the weld provided the required capacity and the section integrity remained intact although deformations were observed in the connections. In addition, the dimensional values specified by the regulations are sufficient and effective for fillet welds used to keep the connection between the end plate and column continuous.

In conclusion, in cases where the local deformation of a joint under bending are prevented, the formula used for the weld thickness defined by the relevant regulation is insufficient. Therefore, additional stresses due to deformations should also be taken into consideration for weld thickness in box beam connections where deformations cannot be adequately controlled.

References

[1] Abi-Saad, G., & Bauer, D. (2006). Analytical approach for shear lag in welded tension members. Canadian Journal of Civil Engineering, 33(4), 384-394.

[2] Cheng, J. J. R., Kulak, G. L., & Khoo, H. A. (1998). Strength of slotted tubular tension members. Canadian Journal of Civil Engineering, 25(6), 982-991.

[3] Cheng, J. R., & Kulak, G. L. (2000). Gusset plate connection to round HSS tension members. Engineering Journal-American Institute Of Steel Construction, 37(4), 133-139.

[4] ÇYTHY (2016). Çelik Yapıların Tasarım, Hesap ve Yapım Esaslarına Dair Yönetmelik.

[5] Design Guide 3, (2009). For Rectangular HollowSection (Rhs) Joints Under Predominantly Static Loading. Comité International Pour Ie Développement Et L'étude De La Construction Tubulaire.

[6] Easterling, W. S., & Gonzales, L. (1993). Shear lag effects in steel tension members. Engineering Journal, 3, 77-89.

[7] Eurocode 3, (2003). Design of steel structures - Part 1-8: Design of joints. European Committee For Standardization, Brussels.

[8] Fenkli, M., Çelik, İ.,D., Kımıllı, N.A., Sivri, M., 2017. "Investigation of Capacity on the Hollow Sections Connections with Stiffening Plate" Advanced Steel Construction., Vol. 3, March 2017. DOI : 10.18057/IJASC.2017.13.1.

[9] Humphries, M. J. R., & Birkemoe, P. C. (2004, June). Shear lag effects in fillet-welded tension connections of channels and similar shapes. In Proceedings of the ECCS/AISC Workshop on Connections in Steel Structures V: Innovative Steel Connections, Amsterdam, The Netherlands (pp. 3-4).

[10] Korol, R. M. (1996). Shear lag in slotted HSS tension members. Canadian Journal of Civil Engineering, 23(6), 1350-1354.

[11] Ling, T. W., Zhao, X. L., Al-Mahaidi, R., & Packer, J. A. (2007). Investigation of shear lag failure in gusset-plate welded structural steel hollow section connections. Journal of Constructional Steel Research, 63(3), 293-304.

[12] Martinez-Saucedo, G., Packer, J. A., & Willibald, S. (2006). Parametric finite element study of slotted end connections to circular hollow sections. Engineering Structures, 28(14), 1956-1971.

[13] Martinez-Saucedo, G., Packer, J. A., & Christopoulos, C. (2008). Gusset plate connections to circular hollow section braces under inelastic cyclic loading. Journal of Structural Engineering, 134(7), 1252-1258.

[14] Martinez-Saucedo, G., & Packer, J. A. (2009). Static design recommendations for slotted end HSS connections in tension. Journal of Structural Engineering, 135(7), 797-805.

[15] Schmidt, L. C., & Morgan, P. R. (2011). Member Ductility and Design Detail of Some Welded Joints. International Journal of Space Structures, 26(3), 155-161.

[16] Willibald, S., Packer, J. A., & Martinez-Saucedo, G. (2006). Behaviour of gusset plate connections to ends of round and elliptical hollow structural section members. Canadian Journal of Civil Engineering, 33(4), 373-383.

[17] Willibald, S., Packer, J. A., Martinez Saucedo, G., & Puthli, R. S. (2004, June). Shear lag in slotted gusset plate connections to tubes. In Proceedings of the ECCS/AISC Workshop, Connections in Steel Structures V: Innovative Steel Connections (pp. 3-5).

[18] Zhao, R. G., Huang, R. F., Khoo, H. A., & Cheng, J. J. R. (2007). Experimental study on slotted rectangular and square hollow structural section (HSS) tension connections. Canadian Journal of Civil Engineering, 35(11), 1318-1330.

[19] Zhao, R., Huang, R., Khoo, H. A., & Cheng, J. R. (2009). Parametric finite element study on slotted rectangular and square HSS tension connections. Journal of Constructional Steel Research, 65(3), 611-621.

[20] Zhao, X. L., Al-Mahaidi, R., & Kiew, K. P. (1999). Longitudinal fillet welds in thin-walled C450 RHS members. Journal of Structural Engineering, 125(8), 821-828.